Biochimica et Biophysica Acta, 604 (1980) 321–345
© Elsevier/North-Holland Biomedical Press

BBA 85211

THE MECHANISM OF THE SODIUM PUMP

DAVID G. LEVITT

University of Minnesota, Department of Physiology, Minneapolis, MN 55455 (U.S.A.)

(Received April 15th, 1980)

Contents

I. Introduction . . . 322

II. A channel as a model for the sodium pump . . . 323

III. The pump model . . . 324
A. The channel subunit . . . 325
B. Kinetics of the dimer . . . 326

IV. Cell flux data . . . 328
A. Sodium-potassium exchange (J_{NK}) . . . 328
B. Sodium-sodium exchange (J_{NN}) and sodium-potassium reversal (J_R) . . . 330
C. Potassium-potassium exchange (J_{KK}) . . . 331
D. Kinetics with zero internal $[K^+]$ . . . 332
E. External binding site – Molecular model and kinetics . . . 332

V. Enzymatic data . . . 334

VI. Simultaneous versus consecutive model . . . 336

Appendix . . . 339

AI. Solution to Scheme I (state S_4 neglected) . . . 339
A. Na-K exchange (J_{NK}) . . . 339
B. Na-K reversal (J_R) . . . 340
C. Na-Na exchange (J_{NN}) . . . 340

AII. Solution with state S_4 included . . . 340
A. K-K exchange (J_{KK}) . . . 341
B. Kinetics of Na-K exchange when the internal $[K^+] = 0$ . . . 341

AIII. Kinetics when multiple occupancy states of the external site are included . . . 342
A. High $[Na^+]$, varying $[K^+]$ . . . 343
B. Zero external $[Na^+]$ with varying external $[K^+]$ . . . 343
C. Flux as a function of the external $[Na^+]$ . . . 344

Acknowledgements . . . 344

References . . . 344

I. Introduction

Much is known about the (Na^+, K^+)-pump [1–4]. The intermediate states of the enzyme have been characterized and the kinetics of many of the transition rates have been established. In addition, the kinetics of the different modes of transport of the intact red cell pump have been investigated in great detail and the concentration dependence and sidedness of action of most of the reactants have been established. Despite this knowledge, a model that provides a quantitative description of both the enzymatic and red cell flux data has not, as yet, been presented. The major difficulty is that the biochemical studies of the enzyme are most consistent with and usually interpreted in terms of a 'consecutive' model where a single transport site passes consecutively between the two sides of the membrane (Fig. 3B), while much of the red cell flux data is not compatible with a consecutive model and, instead, suggests that transport sites are 'simultanously' present on both sides of the membrane. Although several authors have suggested that it should be possible to reconcile this discrepancy with a 'flip-flop' type of model in which two identical subunits are coupled out of phase [1–3,5], this has not been demonstrated quantitatively.

The purpose of this paper is to present a detailed physical mechanism for the sodium pump that is in quantitative agreement with most of the generally accepted enzymatic and red cell flux data. These data are so detailed and extensive that severe constraints are placed on possible models. Although the proposed model cannot, of course, be proved to be unique, it is the only one of the many that were considered that could successfully fit the experimental data. This paper should also provide a detailed review and summary of the features of the pump that must be explained by any successful model.

The model has two features which are very attractive. First, it is kinetically simple – simpler, for example, than the Post-Albers consecutive model. The enzyme cycles through only three kinetic states during the normal operation of the pump and one of the transitions is rate-limiting. This means that it is possible to obtain a complete general kinetic solution for the behavior of the pump in a simple form. The second attractive feature of the model is that it can explain or predict experimental behavior that was not considered when the model was originally developed. This is the case for all results discussed in Section VI. For example, the predicted behavior of the model when the two subunits are uncoupled is in complete agreement with the experimental data on the putatively uncoupled enzyme.

In the first part of the paper (Section II) the results of recent electrostatic calculations on ion channels will be discussed in relation to the sodium pump. It will be shown that a channel that alternates between holding either three Na^+ or two K^+ is compatible with these calculations and provides a simple physical explanation of the experimental stoichiometry and ion interactions of the pump. In Section III, the proposed kinetic model will be described in detail. The model is basically a specific version of the 'flip-flop' type of model – consisting of two identical coupled subunits. The model differs from other versions in that the subunits are coupled only during one of the reaction steps. A unique feature of the model is that it is necessary to assume that the state in which the enzyme is when it is isolated in the presence of Na^+ and the absence of K^+ represents a side reaction that is not involved during the normal operation of the pump (although it is important, for example, in K^+-K^+ exchange). Recently, detailed information about the kinetics of transitions to and from this state has been obtained. It is shown (Section VI) that these kinetics are in good agreement with the predictions of the simultaneous model proposed

here and are not consistent with the consecutive model. In the next two sections it will be shown that the proposed model is consistent with most of the available red cell flux (Section IV) and enzymatic data (Section V). Section VI focuses on three sets of experimental results in which the kinetics predicted by the simultaneous model differ from the predictions of the consecutive model. In each case, the experimental data support the simultaneous model.

II. A channel as a model for the sodium pump

Recently, detailed calculations of the electrostatic energy in multiply occupied membrane channels have been performed [6,7]. The specific calculations were for an uncharged channel resembling that formed by gramicidin (4 Å in diameter and 25 Å long) but the general implications of these results should be applicable to most membrane channels. The results of these calculations suggest that a channel would provide a natural explanation for the stoichiometry and ion interactions of the sodium pump. A detailed schematic representation of the proposed channel model is shown in Fig. 1 and will be discussed in Section III. In this section, qualitative arguments favoring a channel model will be presented.

Probably the most remarkable aspect of the pump is the stoichiometry of three Na^+ pumped out to two K^+ pumped in per ATP split which has been established for the red cell membrane [8] and for reconstituted enzyme purified from shark rectal gland [9], canine brain [10] and canine [11] and ovine [12] kidney. Since there are probably, at most, two catalytic subunits per enzyme and it seems unlikely that a subunit turns over more than once per pump cycle, one must conclude that more than one ion is transported per subunit. A simple physical realization of this (Fig. 1) is an aqueous channel which is

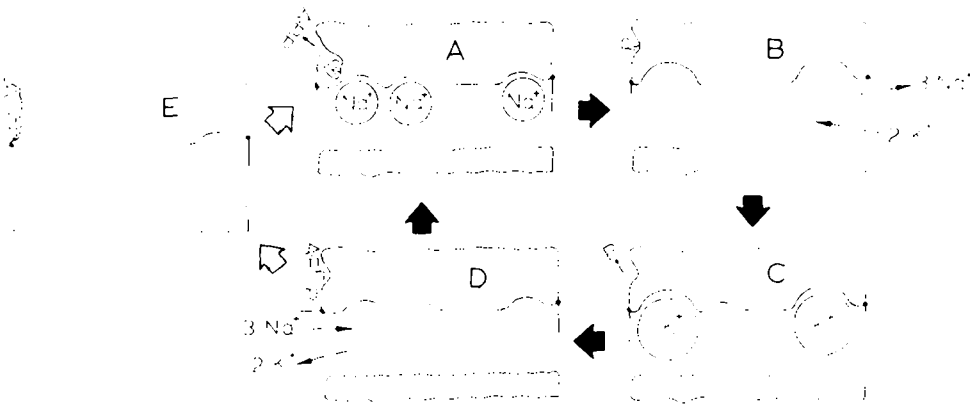

Fig. 1. States of the channel subunit. In subunit D, the channel is open to the inside of the cell and ATP (indicated by the symbol A-P-P-P) is bound with a low affinity. In the transition from D to A, three Na^+ bind to the channel, initiating phosphorylation. In subunit A, the Na^+ are occluded and the bond to phosphate (indicated by the symbol P) is of a high-energy form (represented by the phosphate being buried deep in the enzyme and dehydrated). In the transition from A to B, the phosphate bond becomes a low-energy form (exposed to the aqueous medium) and the Na^+ are released to the external medium. In the transition from B to C, K^+ binds in the channel, initiating dephosphorylation and the occlusion of the K^+. In the transition from C to D, the channel becomes open to the internal medium. This transition is driven by the coupled conformational change that occurs in the other subunit. Subunits A–D (solid arrows) are involved in the normal operation of the pump. The transitions to state E (which has a high affinity for ATP) is a side reaction (see text).

alternatively open to the two sides of the membrane [13] and can hold either three Na^+ or two K^+. The observed stoichiometry would be explained if phosphorylation could occur only when the channel is occupied by three Na^+ and dephosphorylation only when occupied by two K^+ (as shown schematically in Fig. 1).

The electrostatic calculations provide direct support for this simple model. The calculations show that there is relatively little electrostatic interaction between ions placed at opposite ends of the channel. This calculation is supported by experiments on the gramicidin channel which suggest that it can contain two cations [7]. Thus, it is reasonable to assume that a channel can transport at least two ions per cycle. The electrostatic calculations also show that when there are three ions in the channel there is a very large repulsive energy of interaction [7]. This energy is reduced by about $7\,kT$ (about one-half the energy available from the hydrolysis of ATP) when a counterion is placed near the channel mouth. This result suggests a simple explanation for the requirement that the channel must be occupied by three Na^+ before phosphorylation can occur. The addition of the third Na^+ would induce a conformational change (driven by an energy of about $7\,kT$) in which a negatively charged group is brought near to the channel mouth. This conformational change would be a requirement for phosphorylation. Finally, if it is assumed that, for steric reasons, it is possible to place three ions in the channel only if they are all Na^+, then one would have a physical explanation of the absolute requirement for Na^+ for phosphorylation. There are a number of ways to explain the requirement for K^+ (or one of its analogs) for dephosphorylation. The one chosen here is based on the assumption that there is a site in the channel (in state B, Fig. 1) that has a high affinity for Na^+ which must be displaced before dephosphorylation can occur. Under physiological conditions, this displacement is the result of the binding of two K^+ per channel. This condition for dephosphorylation was chosen because it provides a physical explanation for the complex ion interactions that occur at the external site (see subsection IVE for details).

One of the main advantages of a multiply occupied channel over independent ion sites is that it provides a physical explanation for ion interactions. For example, it is well established that K^+ inhibits the action of Na^+ at the internal site [14]. This is difficult to explain on the basis of independent sites, since it would mean that the binding of Na^+ to an ion site stimulated phosphorylation while the binding of K^+ inhibited it. This seems unlikely, since one would expect that the dominant effect of ion binding would be electrostatic and would be similar for Na^+ and K^+. However, this inhibition is a natural consequence of a multiply occupied channel, since the presence of a K^+ in the channel would sterically prevent the placing of a third ion in the channel and would block phosphorylation.

Although these arguments provide only suggestive evidence for a channel mechanism, this model provides such a simple and natural way of handling the kinetics that it will be assumed for the kinetic model. However, the validity of the kinetics does not depend on this assumption.

III. The pump model

The proposed model, which consists of two identical coupled subunits, will be described in two parts. First, the states and reaction steps of the individual subunit (channel) will be described (Fig. 1), and then the kinetics of the complete dimer will be presented in terms of the coupled subunit states (Figs. 2 and 3A). The Post-Albers scheme is used as the prototype of the consecutive models [15,16]. Most consecutive models, such

as that recently proposed by Karlish et al. [17], are kinetically equivalent to the Post-Albers scheme. It will be shown that the corresponding states in Fig. 3 have the same enzymatic properties and, therefore, all the enzymatic data that have been used to support the Post-Albers scheme are just as consistent with the simultaneous model proposed here.

IIIA. The channel subunit

The basic sequence and states of the subunit are essentially the same as those proposed by Karlish et al. [17] for the complete enzyme. It is assumed that the subunit can exist in five different states which are shown schematically in Fig. 1. The channel can be in equilibrium with the internal solution (states D and E), the external solution (state B) or occluded (states A and C) as indicated by swinging doors at the ends of the channel. The opening and closing of the doors correspond to conformational changes that sterically block the movement of ions. The actual movement does not have to be very large, since a shift of only about 2 Å is enough to block the passage of an ion. In state A, the channel contains three Na^+ in an occluded state and has a high-energy phosphate bond (as indicated by the fact that it can reversibly form ATP by combining with ADP). As discussed above, there must be a negatively charged group near the channel end when the channel contains three cations. In Fig. 1 this group is represented by phosphate itself, although this is not necessary. In the transition from state A to B, a conformational change occurs in which: (a) the channel becomes open to the external solution; (b) the affinity for Na^+ is greatly reduced and (c) the phosphate bond becomes low in energy as indicated by its ability to be formed from P_i. Taniguchi and Post [15] have pointed out that one of the main energy-requiring steps of the pump is the change in Na^+ affinity that occurs in this step. This energy is supplied by the change in the phosphate bond from a high- to a low-energy bond. Much of the energy released by the splitting of ATP is utilized in this step. This change in energy state is presumably the result of just a conformational change, since there is no evidence of a chemical change in the bond. One physical explanation for the change in energy is that in the high-energy state the phosphate is buried deep in the enzyme, dehydrated and surrounded by low dielectric material while in the low-energy state, the phosphate becomes exposed to water [18]. This is shown schematically in Fig. 1. Much of the decrease in Na^+ affinity can be accounted for by the movement of the negatively charged group (represented by phosphate in Fig. 1) away from the channel mouth with the resultant increase in electrostatic repulsion between the Na^+.

It is assumed that the central site in state B has a relatively high affinity for Na^+ and dephosphorylation can occur only when Na^+ is displaced from this site, as occurs, for example, when a K^+ binds to the left end site. This competition for ions at the external site is examined in detail in subsection IVE where it is shown that this model is in quantitative agreement with the experimental kinetics. In the transition from state B to C, K^+ displaces the central Na^+ and dephosphorylation occurs, accompanied by a conformational change in which the two K^+ become occluded. In the transition from state C to state D, a conformational change occurs in which (a) the channel becomes open to the internal solution and (b) the affinity for K^+ is greatly reduced. As was the case for the transition from A to B, this change in affinity is energetically unfavorable. This reaction (state C to D) is driven by the phosphorylation (transition from D to A) which occurs simultaneously in the other subunit channel and is obligatorily coupled to this transition (see below for details). State D has a low-affinity binding site for ATP and can undergo

transitions to two different states: the transition to state A (which is involved in the normal operation of the pump) in which phosphorylation occurs (dependent on the binding of three Na^+), or the transition of state E which has a high affinity for ATP. State E can also be phosphorylated and converted to state A.

IIIB. Kinetics of the dimer

The states of the complete enzyme (dimer) are shown in Fig. 2. The kinetic scheme for the dimer is shown in Fig. 3A and the corresponding states of the Post-Albers scheme are shown in Fig. 3B. In state S_1, one subunit is in state D and one in state A. This corresponds to E_1P of the Post-Albers scheme. In the transitions from S_1 to S_2 and S_2 to S_3, only the upper subunit in Fig. 2 is involved, and its changes are identical to those of the corresponding single state of the Post-Albers scheme (Fig. 3B). The critical difference in the two models is in the transition from S_3 to S_1 (or, in the Post-Albers scheme, E_2 to E_1P). For the simultaneous model during the normal operation of the pump (Na-K

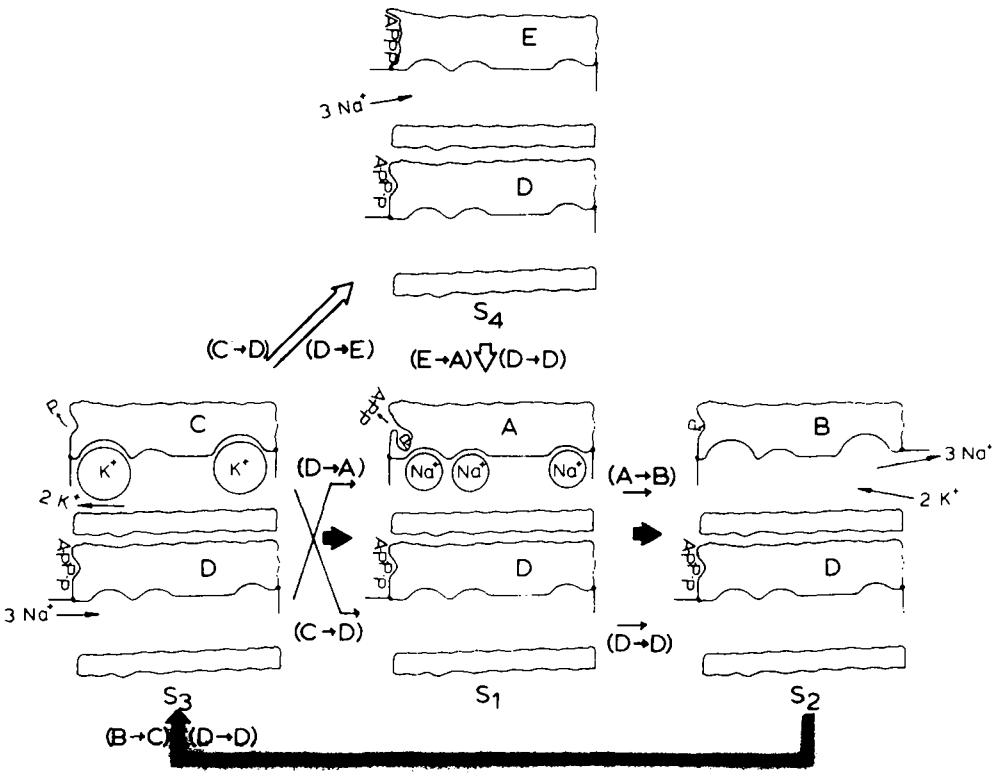

Fig. 2. States of the enzyme dimer. In state S_1, one subunit is in state A and the other in state D. In the transitions from S_1 to S_2 and S_2 to S_3, only the upper subunit is involved. The transition from S_3 to S_1 involves a coupled conformational change in which subunit D of S_3 becomes phosphorylated and converted to A of S_1 while, simultaneously, C of S_3 is converted to D of S_1. The transition from S_3 to S_4 (open arrows) is a side reaction involving a coupled conformational change in which ATP binds to subunit D of S_3 with a high affinity, converting it to subunit E of S_4, while, simultaneously, subunit C of S_3 is converted to subunit D of S_4.

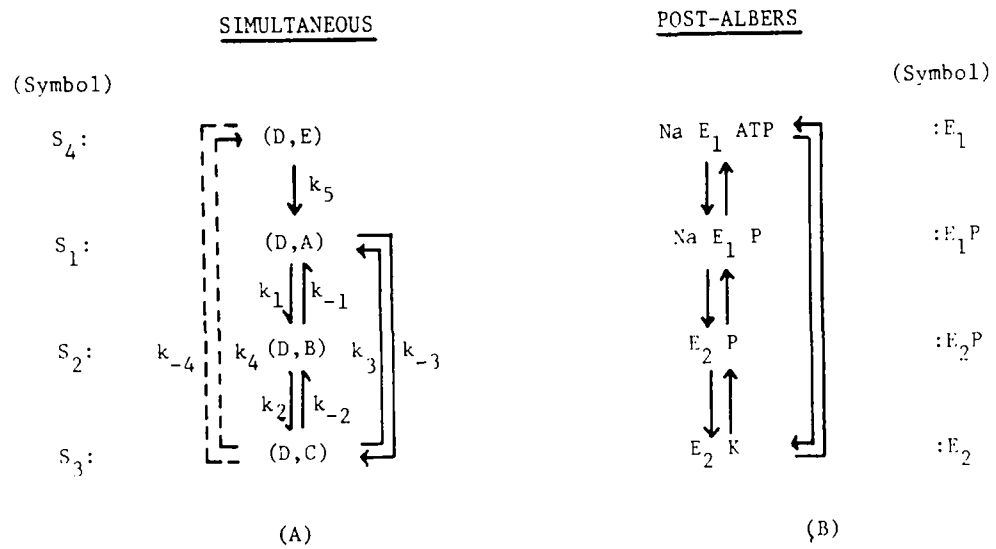

Fig. 3. Comparison of the kinetics of (A) simultaneous and (B) consecutive (Post-Albers) models. The corresponding states of the two models are in the same row. The normal cycle of the simultaneous model is indicated by the solid arrows while the dashed arrows indicate a side reaction (see text). The states (S) of the simultaneous model correspond to those in Fig. 2 and the subunits (A + E) correspond to those in Fig. 1.

exchange, solid arrows, Fig. 2), there is a coupled transition of the two subunits in which the channel in state D of S_3 is phosphorylated and converted to state A of S_1, while state C of S_3 is converted to state D of S_1. As indicated above, the energy required to convert state C to D is provided by energy released during the phosphorylation involved in the transition from D to A. The transition to S_4 (Figs. 2 and 3A) is essentially a side reaction. In this transition, the energy required to convert C (of S_3) to D (of S_4) comes from the increase in the binding affinity (deeper energy well) of ATP that occurs in the coupled transition of state D (of S_3) to state E (of S_4). It will be assumed that if the internal $[K^+]$ is above about 10 mM, then the equilibrium between S_4 and S_3 is far towards S_3 so that under the usual conditions in which the pump flux is measured (high internal $[K^+]$) the fraction of the pump that is in state S_4 is negligible. State S_4 does become important under some conditions. For example, when the enzyme is prepared in the absence of K^+ (which is often the initial state in enzyme kinetic studies), most the enzyme will be in state S_4. Also, as will be shown below, S_4 is involved in K-K exchange and become important when Na-K exchange is measured with low internal $[K^+]$ (as in the experiments of Sachs [19]).

When S_4 is negligible, the kinetics can be written in the form:

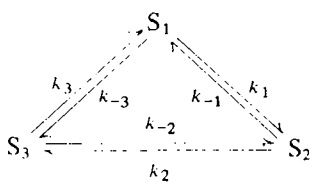

Scheme I.

Since there are only three kinetic states, the kinetic solution is quite simple. The general solution for the various kinetic conditions is presented in the Appendix and, usually, only the final result will be shown in the text.

IV. Cell flux data

The theoretical significance of the red cell flux studies was first pointed out by Hoffman and Tosteson [20]. These data have been extended and well summarized by Garrahan and Garay [21]. The significance of these experiments can be summarized by two statements that have very important implications about possible models of the sodium pump. First, the red cell flux (J) for all the different transport modes of the pump (Na-K exchange, Na-K reversal, Na-Na exchange and, probably, K-K exchange) can be described by an equation of the form:

$$J = X(a^i_K, a^i_N) \cdot Y(a^o_K, a^o_N) \tag{1}$$

where X and Y are general functions of the Na^+ (a_N) and K^+ (a_K) activities. The superscripts, o and i, indicate extracellular and intracellular activity, respectively. Eqn. 1 implies that the concentration dependences of the inner and outer sites are independent of each other. This condition (if correct) places severe restrictions on any possible model. For example, a consecutive model cannot, even approximately, satisfy Eqn. 1 and is therefore immediately excluded. As discussed by Garrahan and Garay [21] and illustrated for the model proposed in this paper (see Appendix), this condition also places important constraints on possible simultaneous models. The second conclusion of these red cell flux experiments is that the apparent Na^+-concentration dependence of the inner site is the same for Na-K exchange and Na-Na exchange and the Na^+-concentration dependence of the outer site is the same for Na-Na exchange and Na-K reversal [21]. In contrast, the K^+-concentration dependence of the inner site for K-K exchange is markedly different from that for Na-K reversal [22]. These relationships place important additional restrictions on the possible models.

The evidence supporting Eqn. 1 is based primarily on the experiments of Hoffman and Tosteson [20] and Garay and Garrahan [14]; experiments in which a significant amount of K^+ was present in the cell. Sachs [19] and Chipperfield and Whittam [23] have investigated the kinetics of Na-K exchange for the case where the internal [K^+] was very low and found that the concentration dependence of the external site for K^+ varied with the internal Na^+ concentration. It will be shown that this result of Sachs [19], which is an exception to Eqn. 1, is also consistent with the model proposed here.

IVA. Sodium-potassium exchange (J_{NK})

It is shown in the Appendix that in order to satisfy Eqn. 1 it is necessary to assume for Scheme I that: (1) k_3 and k_{-3} are much less than k_1 and (2) k_3 and k_{-3} are much less than k_{-2}. These assumptions mean that the rate-limiting step for Na-K exchange is the transition from S_3 to S_1 and that most of the enzyme is either in state S_3 or S_2 (which is effectively in equilibrium with S_3). It will be shown below that these assumptions are in rough agreement with the enzymatic results. With these two assumptions, the rate of Na-K exchange can be written in the form (Appendix, Eqn. 7A):

$$J_{NK}/S = \alpha_1\alpha_2\alpha_3 f(a^i_N|a^i_K)g(a^o_K|a^o_N)/D(a^o_N, a^o_K)$$
$$D = \alpha_1\alpha_{-2} + \alpha_2\alpha_1 g(a^o_K|a^o_N) + \alpha_{-1}\alpha_{-2}h(a^o_N|a^o_K) \tag{2}$$

where S is the total amount of enzyme, $f(a_N^i|a_K^i)$ is the fraction of the internal sites (state D) occupied by three Na^+ when the internal Na^+ and K^+ activities are a_N^i and a_K^i, $g(a_K^o|a_N^o)$ and $h(a_N^o|a_K^o)$ are the fractions of the external sites (state B) occupied by two K^+ or by three Na^+, respectively; and the α terms are rate constants that are independent of cation activity. It can be seen that Eqn. 2 is of the form of Eqn. 1. It is useful to consider the simple case in which binding at the inner and outer sites can be described by a simple Michaelis constant:

$$f(a_N^i,a_K^i) = a_N^i/(a_N^i + K_N) : \quad g(a_K^o|a_N^o) = a_K^o/(a_K^o + K_K) \tag{3}$$

If, in addition, k_{-1} is negligible (which should be true under most conditions) then Eqn. 2 can be written as:

$$\begin{aligned} J_{NK}/S &= V[a_N^i/(a_N^i + K_N)][a_K^o/(a_K^o + K_K^{ap})] \\ K_K^{ap} &= \alpha_{-2}K_K/(\alpha_{-2} + \alpha_2) : \quad V = \alpha_3\alpha_2/(\alpha_{-2} + \alpha_2) \end{aligned} \tag{4}$$

Eqn. 4 is of the form of the product of simple independent binding reactions at the inner and outer surfaces of cell. The apparent binding constant at the inner site is equal to the true binding constant, while the relationship of the apparent binding constant at the outer site (K_K^{ap}) to the true constant (K_K) is described in Eqn. 4.

Garay and Garrahan [24] have shown that the rate of Na-K exchange varies with the ATP concentration in the millimolar range and that the apparent affinity of the internal site for Na^+ and that of the external site for K^+ are independent of the ATP concentration. This is in agreement with the model predictions, since ATP should affect only the rate α_3 through binding to the low-affinity (millimolar range) site on S_3 and should not affect the apparent dissociation constants (see Eqn. 2 or Eqn. 4). At very low ATP concentrations, a 'high-affinity' ATP component of the cell flux [36] and of the $(Na^+ + K^+)$-ATPase [29,55,56] is observed. This is consistent with the model if a slow transition from S_3 to S_4 can occur in the absence of ATP binding to S_3. This reaction would be negligible at physiological levels of ATP but would become important at very low ATP levels when the phosphorylation of the high-affinity site on S_4 is the dominant reaction. An increase in the internal $[K^+]$ should shift the equilibrium of reaction 4 towards S_3 (with a low ATP affinity) and therefore decrease the reaction rate at low levels of ATP. This was observed experimentally by Neufeld and Levy [55] who found that K^+ inhibited the high-affinity ATP component with an apparent K_m of about 10 mM.

Garay and Garrahan have also shown that increasing the $[P_i]$ from a control value of about 1 mM to about 24 mM produces an inhibition of about 50% of Na-K exchange and does not affect the apparent ion affinities. This presents a contradiction to the predictions of the model, since the apparent dissociation constant of the external site for K^+ should decrease with increasing phosphate levels because α_{-2} should depend on the amount of phosphate bound to S_3 (see Eqn. 4). One possible explanation is that S_3 is nearly saturated with phosphate at the lowest concentration investigated (1 mM) and therefore α_{-2} will be relatively independent of phosphate concentration over the range studied. The 50% inhibition in the rate of Na-K exchange when the phosphate level is raised from 1 to 24 mM would then have to be explained by an action of phosphate at some step other than the transition from S_3 to S_2. This is supported by the observation that phosphate produces a greater inhibition of the Na^+-ATPase enzymatic reaction in the absence of K^+ (when the transition from S_3 to S_2 is not involved) than of the $(Na^+ + K^+)$-ATPase [25].

IVB. Sodium-sodium exchange (J_{NN}) and sodium-potassium reversal (J_R)

The comparison of these two transport modes provides an important argument against the Post-Albers scheme and in favor of the simultaneous model. It is shown in Section VI that in the Post-Albers scheme the same reaction steps that limit Na-K reversal should also limit Na-Na exchange and, therefore, the Post-Albers scheme predicts that Na-Na exchange and Na-K reversal should occur at roughly the same rate. However, the rate of Na-Na exchange is relatively fast (about 1/4 the rate of Na-K exchange [14]) and more than 10-times faster than Na-K reversal (see Section VI), suggesting that Na-Na exchange does not involve the slow step that limits Na-K reversal. This is avoided in the simultaneous model (Scheme II) were it is assumed that Na-Na exchange proceeds through a coupled reaction step in which one subunit is phosphorylated from ATP while, simultaneously, the other subunit forms ATP from ADP and phosphate – so that the overall free energy change is zero. This argument for the simultaneous model is described in more detail in Section VI.

The proposed mechanism for Na-Na exchange, which is a natural extension of the kinetic model shown in Fig. 2, is depicted in Scheme II:

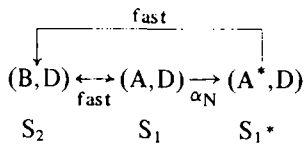

Scheme II.

The cycle begins, for example, when three Na^+ from the external solution enter state B of S_2, converting it to S_1. It is assumed that this step is relatively fast and reversible so that S_2 and S_1 are effectively in equilibrium. The rate-limiting step (α_N) is the coupled conformational change of the subunits where internal Na^+ binds to state D of S_1 which becomes phosphorylated and converted to state A while, simultaneously, state A is converted to state D (forming ATP from ADP and phosphate) releasing the occluded Na^+ (which came from the external medium) to the internal medium. The cycle is completed when the new state A^* of S_1^* (the asterisk indicates that the occluded Na^+ came from the inside medium) rapidly equilibrates with the external medium (through S_2) forming S_1. Although the transition between S_1 and S_1^* brings about Na-Na exchange, these two states are kinetically identical to the single state S_1 in Scheme I.

The rate of Na-Na exchange is described by (Appendix, Eqn. 13A):

$$J_{NN}/S = \alpha_N S_1^N/S = \alpha_N \alpha_{-1} \alpha_{-2} f(a_N^i | a_K^i) h(a_N^o | a_K^o)/D \tag{5}$$

In order for the transition from S_1 to S_1^* to occur, ATP must be bound to subunit D and ADP must be bound to subunit A of S_1. This is consistent with the experimentally observed dependence of the Na-Na exchange rate on the ADP [26] and ATP [27] concentrations.

The rate of Na-K reversal is equal to the flux in the reverse direction through the cycle of Scheme I (Appendix, Eqn. 9A):

$$J_R/S = \alpha_{-1} \alpha_{-2} \alpha_{-3} r(a_K^i | a_N^i) h(a_N^o | a_K^o)/D \tag{6}$$

where $r(a^i_K|a^i_N)$ is the fraction of the internal sites (state D) occupied by two K^+. It can readily be seen that Eqns. 5 and 6 are of the form of Eqn. 1. Also, as has been observed experimentally: (1) the concentration dependence of the internal site for Na^+ in Na-Na exchange ($f(a^i_N|a^i_K)$, Eqn. 5) is identical to that for Na-K exchange (Eqn. 2); and (2) the concentration dependence of the external site for Na^+ in Na-Na exchange ($h(a^o_N|a^o_K)/D$, Eqn. 5) is identical to that for Na-K reversal (Eqn. 6).

IVC. Potassium-potassium exchange (J_{KK})

Since the K^+ in S_3 is occluded, K-K exchange must involve a transition to either S_1 or S_4 and then back to S_3. Since the transition from S_1 to S_3 is very slow (as indicated by the low rate of Na-K reversal, see below), the primary mechanism must be through S_4:

$$(D, E) \underset{k_4}{\overset{k_{-4}}{\rightleftharpoons}} (D, C) \rightleftharpoons (D, B)$$

S_4 S_3 S_2

Scheme III.

The equilibrium of reaction 4 is far towards S_3 so that if there is a significant level of internal K^+, only a negligible fraction of the enzyme will be in state S_4. As in the case of Na-K exchange, it is assumed in Scheme III that the exchange between S_3 and S_2 is fast. This assumption is consistent with the enzymatic results (see Section V). The kinetics for the general case when S_4 is included in the reaction cycle are given in Appendix (Eqn. 19A). For the case where internal $[Na^+]$ is zero and external $[K^+]$ is high, the rate of K-K exchange is given by (Appendix, Eqn. 20A):

$$J_{KK}/S = k_{-4}S_4/S = \alpha_4 k_{-4}/(k_{-4} + \alpha_4) : \qquad k_{-4} = \alpha_{-4} r(a^i_K|a^i_N) \tag{7}$$

Eqn. 7 is again of the form of Eqn. 1.

Experimentally and, as was shown above, theoretically, the affinity of the internal site for Na^+ is the same in Na-K and Na-Na exchange. In contrast, the apparent dissociation constant of the internal site for K^+ during K-K exchange is about 1/30 of that found during Na-K reversal [28,29]. It can be shown that these different dissociation constants for K^+ are a natural consequence of the reaction mechanism proposed here. Assume that $r(a^i_K|a^i_N)$ has the simple form:

$$r(a^i_K|a^i_N) = a^i_K/(a^i_K + K) \tag{8}$$

where K is the true Michaelis-Menten constant of the internal site for K^+. Substituting Eqn. 8 into Eqn. 7 and rearranging:

$$J_{KK}/S = [\alpha_4\alpha_{-4}/(\alpha_{-4} + \alpha_4)]\,[a^i_K + K^{ap})] : \qquad K^{ap} = \alpha_4 K/(\alpha_4 + \alpha_{-4}) \tag{9}$$

where K^{ap} is the apparent Michaelis-Menten constant for K-K exchange. The ratio α_4/α_{-4} is the equilibrium constant for reaction 4 (Scheme III). If, as will be assumed, this equilibrium is far towards S_3, then $\alpha_4/\alpha_{-4} \ll 1$ and $K^{ap}/K \simeq \alpha_4/\alpha_{-4} \ll 1$. That is, the apparent Michaelis-Menten constant for K-K exchange (K^{ap}) is much less than the apparent constant for Na-K reversal (K; see Eqns. 6 and 8). The experimental value of K^{ap} for K-K exchange is about 10 mM [28] while K for Na-K reversal (which is equal to the K_m value of S_4 or S_1 for K^+; Eqn. 6) is about 300 mM [29], so that the equilibrium constant for

reaction 4 (α_4/α_{-4}) is about 0.03. This value of K^{ap} is approximately equal to the value found for the inhibition by K^+ of the high ATP-affinity component of the ATPase reaction (Ref. 55; and see subsection IVA) as predicted by the model.

These results are in good agreement with the experimental results of Karlish et al. [17]. They measured the transition rate between S_4 and S_3 (which they interpreted in terms of $E_1 \rightarrow E_2$ in the Post-Albers notation) and obtained results that suggested that S_4 had a low affinity for K^+ and that the equilibrium between S_4 and S_3 was far towards S_3. This is just what was predicted above. The above theoretical calculations are only qualitative because in the experiments in which the apparent K_m values for Na-K reversal and K-K exchange were determined the internal [Na^+] was not zero (as is assumed in Eqn. 7) and was probably high enough to compete with K^+. The kinetics for the general case are described in Appendix.

The rate of K-K exchange is proportional to the rate constant α_4 (Eqn. 7) which depends on the binding of ATP to the low-affinity site on S_3. This is in agreement with the experimental dependence of K-K exchange on the internal concentration of ATP (or its analogs, including compounds that cannot phosphorylate the enzyme [28,30]). It was assumed in the derivation of Eqn. 7 that the exchange between S_3 and S_2 was fast. Since this rate depends on the P_i in the cell, the model is consistent with the experimental P_i-concentration dependence of K-K exchange [28].

IVD. Kinetics with zero internal [K^+]

Sachs [19] investigated the kinetics of Na-K exchange under conditions when the external [Na^+] and internal [K^+] were close to zero. He found, in contrast to the results of Hoffman and Tosteson [20] and Garay and Garrahan [14] and the predictions of Eqn. 1, that the apparent affinity constant of the external site for K^+ had a strong dependence on the internal [Na^+] (Chipperfield and Whittam [23] have also observed this internal [Na^+] dependence under similar conditions, although their results differed significantly from those of Sachs). This inconsistency with Eqn. 1 can be explained by the zero internal [K^+] in these experiments which significantly increases the fraction of the enzyme that is in state S_4 (see Fig. 1). It is shown in Appendix that the model predictions are in qualitative agreement with the results of Sachs. A quantitative fit of the theory to the data of Sachs indicates that the K_m value for Na^+ at the internal site is about 1 mM for S_3 and about 10 mM for S_4. This K_m for S_3 is in rough agreement with the experimental K_m for internal Na^+ [14] during Na-K exchange when internal K^+ is present so that most of the enzyme is in state S_3 (see Eqn. 4). The higher K_m value for S_4 is also in agreement with the K_m for Na^+ of about 8 mM determined from the initial rate of phosphorylation of the enzyme [31] or from the rate of ATP-ADP exchange in *N*-ethylmaleimide-treated enzyme [32]. Since this rate is measured in the absence of K^+, all the enzyme is initially in state S_4 and therefore this K_m should be that for S_4.

IVE. External binding site – Molecular model and kinetics

Since the channel can hold up to three Na^+, two K^+ and various combinations of Na^+ and K^+, there should be a large number of different occupancy states of the channel. These various states should manifest themselves in, for example, the kinetics of Na-K exchange as a function of the external Na^+ and K^+ concentrations. The purpose of this section is to present a specific molecular model of the channel that provides a quantitative

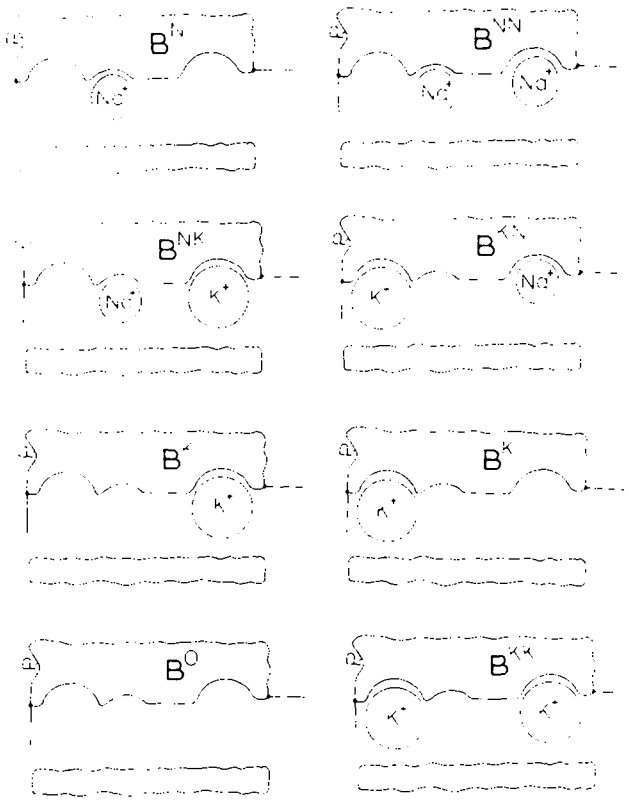

Fig. 4. Possible occupancy states of the B subunit of state S_2. The central site has a high affinity for Na^+ and dephosphorylation can occur only when there is no ion at this site. The different states are labeled by the superscript on B.

description of the known kinetics at the external site. The model presented here is essentially a physical realization of the kinetic model (slightly modified) proposed by Sachs [33].

As shown in Fig. 1, the channel open to the external solution (state B) is assumed to have three sites – one at each end and a more central site close to the left end. The central site is particularly important because it will be assumed that it has a relatively high affinity for Na^+ and that dephosphorylation ($S_2 \rightarrow S_3$) can occur only if there is no ion at this site. The allowed occupancy states of this channel are shown schematically in Fig. 4. The allowed states are limited by the assumption that a K^+ at the left end site prevents binding of an ion at the central site. Thus, dephosphorylation (and transport) can occur only for the four states of Fig. 4 which do not have an ion at the central site: S_2^O (empty) which is responsible for the uncoupled sodium efflux that is observed in red cells; S_2^K (two states) and S_2^{KK}, states containing one or two K^+ (or its analogs), and S_2^{KN}, a state that has a K^+ at the left end and an Na^+ at the right end. (The superscripts on S_2 refer to the status of the B subunit channel shown in Fig. 3.)

The quantitative kinetics for the model are described in the Appendix. Only the qualitative results will be discussed here. For the normal physiological condition (high external $[Na^+]$ and relatively high $[K^+]$) the only state present in a significant amount that can be

dephosphorylated is S_2^{KK}, and, therefore, two K^+ are pumped into the cell per cycle. If both K^+ and one of its analogs are present (e.g., Rb^+), the pump will transport the different combination of K^+ and Rb^+ (KK, KRb and RbRb) and the effect of the two ions will be additive, as shown experimentally by Sachs [34]. In the absence of external Na^+ or K^+, state S_2^0 is present and is dephosphorylated, producing the uncoupled Na^+-efflux mode of operation of the pump [36]. For the case of zero external [Na^+] and low [K^+], states S_2^K and S_2^{KK} will be present and there will be transport of either one or two K^+ per pump cycle, as suggested by the data of Sachs [33]. The state S_2^{KN} is a new and unusual state in which one Na^+ and one K^+ are pumped into the cell per cycle. Since the affinity of Na^+ for the right end of the channel is very low compared to that of K^+, this state only becomes important at very low K^+ concentrations and high Na^+ concentrations. It is shown in Appendix that this transporting state, which is a natural consequence of the channel model, provides a simple physical explanation for the [Na^+] dependence of the K^+ flux that is seen at very low K^+ concentrations [33,35] and was interpreted by Cavieres and Ellory [35] in terms of allosteric inhibition.

A general solution for the Na-K exchange kinetics taking account of all the external states of Fig. 4 is given in Appendix. For each of the different occupancy states (S_2^i), there are corresponding rate constants (k_2^i, k_{-2}^i and k_3^i) which enter the final rate equation. It is shown in Appendix that the kinetics for this model are consistent with all of the following experimental results: (1) At high external sodium concentrations (the physiological condition), the dependence of Na-K exchange on the K^+ concentration has the well established sigmoid-shaped plot and only the state where two K^+ are in the external site makes a significant contribution to the flux. (2) At zero external sodium concentration, the dependence of Na-K exchange on external [K^+] can have a sigmoid, hyperbolic or antisigmoid plot, depending on the relative values of the rate constants. (3) At moderate values of external [K^+], a plot of the $(\text{flux})^{-1}$ vs. external Na^+ activity has a linear dependence on the [Na^+] while (4) at very low values of external [K^+], the plot tends to level off, in agreement with the experimental results.

The uncoupled Na^+ efflux from red cells (measured in the absence of external K^+) has a complicated dependence on the external [Na^+] – being inhibited by low concentrations and stimulated by high concentrations [36]. In terms of the model presented here, the inhibition at low concentrations is the result of Na^+ occupying the central site and blocking dephosphorylation. In order to explain the stimulation at high concentrations, a new effect must be invoked. At high concentrations of external Na^+, the channel in state B will tend to be filled by three Na^+ which will cause a transition from state S_2 back to S_1. Since ADP is not present in these experiments, a transition such as that which occurs in Na-Na exchange (Scheme II) cannot occur. Instead, it is necessary to assume that the enzyme in state S_1 has a finite rate of spontaneous dephosphorylation producing the transition $S_1 \rightarrow S_3$ and this accounts for the increased rate of uncoupled Na^+ efflux at high external Na^+ concentrations. This model is also consistent with measurements of the rate of ATP hydrolysis [31,32] and ATP-ADP exchange [32] measured in the absence of K^+.

V. Enzymatic data

As mentioned in Introduction, there is a large amount of information available about the enzymatic behavior of the sodium pump and any proposed model should be consistent with these data. Instead of reviewing all the biochemical results and demonstrating

their consistency with the model proposed here, one can take the following short-cut. Nearly all the enzymatic data have been shown to be consistent with the relatively simple Post-Albers scheme (Fig. 3B). In this section it will be shown that the enzymatic behavior of the proposed model (Fig. 3A) is equivalent to the Post-Albers scheme.

The corresponding states of the proposed model and the Post-Albers scheme are shown in Fig. 3. Both the states S_3 and the corresponding E_2 of the Post-Albers scheme contain an occluded K^+, can be phosphorylated by P_i and have a low affinity for ATP. Both S_1 and the corresponding E_1P have a high-energy phosphate. Both S_2 and E_2P have a low-energy phosphate and can be dephosphorylated by K^+.

The major difference in the two schemes is in the role played by S_4 and the corresponding E_1. For the simultaneous model, S_3 can be directly phosphorylated in the presence of Na^+ and converted to S_1, while in the consecutive Post-Albers scheme, E_2 first goes to E_1 (which has the high affinity for ATP that characterizes S_4) which is then phosphorylated to E_1P. The transition of the enzyme between states E_2 and E_1 has been studied in great detail. The fraction of the enzyme in the two states has been determined, for example, by measuring the enzyme fraction (E_1) that has a high affinity for ATP [37] or formycin triphosphate [38], or that can be rapidly phosphorylated at low ATP concentrations [39] and by measuring the enzyme fraction (E_2) that can be phosphorylated by P_i [5], or catalyze phosphate-oxygen exchange [40], and from tryptophan fluorescence [41]. For all these measurements, the enzyme is initially prepared under conditions where phosphorylation (transition to S_1) is prevented (usually by the absence of Mg^{2+}) so that, in terms of the simultaneous scheme (Fig. 3A), what is being measured is the fraction of the enzyme in states S_3 and S_4. Since S_3 and S_4 have exactly the same enzymatic properties as the corresponding E_2 and E_1, respectively (ability to be phosphorylated by ATP or phosphate, affinity for ATP, etc.), all these studies are consistent with the simultaneous scheme proposed here. For example, all these measurements show that K^+ shifts the equilibrium between E_1 and E_2 towards E_2 and Na^+ shifts the equilibrium towards E_1. In terms of the Post-Albers scheme, these shifts are the result of competition between Na^+ and K^+ for binding to E_1 with K^+ binding shifting the equilibrium towards E_2. In terms of the simultaneous model, these shifts are the result of competition between Na^+ and K^+ for state D of S_4. Since the binding of Na^+ to just one site in the channel (the central site) would be sufficient to block the transition from S_4 to S_3, this model is consistent with recent measurements that suggest that Na^+ and K^+ are competing for a single site [42].

In addition to the above qualitative enzymatic properties of the model, the quantitative enzymatic rates are, at least, in rough agreement with the assumptions of the model. A basic assumption that was made in the derivation of the kinetics was that $k_3 \ll (k_{-2}$ and $k_1)$ which means that the transition from S_3 to S_1 (Scheme I) is rate-limiting, and in the steady state most of the enzyme should be either in state S_3 or S_2 (which is nearly in equilibrium with S_3). The most direct evidence that $k_3 \ll k_{-2}$ comes from the measurement of the phosphate-oxygen exchange. This exchange rate, which presumably involves the transition between S_3 and S_2 and is therefore proportional to k_{-2}, is about 20-times faster than the rate of ATP hydrolysis [40]. This implies that k_{-2} is of the order of 20-times larger than k_3. The evidence in favor of the assumption that $k_3 \ll k_1$ is not as strong. In the absence of phosphate (so that $k_{-2} = 0$) and in the presence of saturating levels of K^+ (so that k_2 is large), all the enzyme should be in the dephosphorylated form S_3 if $k_3 \ll k_1$ (because of the high $[K^+]$, the enzyme in state S_4 can be neglected). Experimentally, under these conditions, about 75% of the enzyme is in the dephosphorylated form in the steady state [43,44]. This indicates that k_1 is about 3-times as

large as k_3. This rough calculation is in general agreement with the quantitative determination of the rate constant by a computer fit to the complete kinetic cycle [16]. A k_1 that is 3-times larger than k_3 would, at least to a first approximation, satisfy the above assumption. In addition, the relative values of the rate constants for the intact red cell membrane may differ considerably from the values for the isolated enzyme.

VI. Simultaneous versus consecutive model

The main argument for the consecutive model (in particular, the Post-Albers scheme) is that it provides such a simple explanation for almost all the enzymatic results. Since only three states are involved in the normal operation of the simultaneous model proposed here (Scheme I), the kinetics are actually simpler than those of the Post-Albers scheme which has four states. Garrahan and Garay [21] have reviewed some of the evidence that favors the simultaneous model. Although the most direct evidence is provided by the red cell flux data (Eqn. 1), additional biochemical evidence is also discussed. The purpose of this section is to examine critically the implications of the two opposing kinetic schemes (described in Fig. 3) and present additional arguments that provide, I believe, strong support for the simultaneous model.

In order to distinguish between the two models, one must look at those reactions in the proposed model which depend on simultaneous binding at both ion sites. There are at least three such steps for which experimental evidence can be obtained: (1) the transition from S_3 to S_1; (2) the reverse transition, from S_1 to S_3; and (3) the transition involved in Na-Na exchange (Scheme III). It will be shown that for each of these transitions, the currently available data seem to support the simultaneous model.

The kinetics of the transition that corresponds to E_2 to E_1 in the Post-Albers scheme and to S_3 to S_4 in the simultaneous model have been measured using either tryptophan fluorescence [43] or formycin-ATP binding [38]. The transition rate was approximately proportional to the ATP concentration, becoming very slow at low [ATP] (about 1 s^{-1} at 10 μM ATP) and could be described quantitatively by assuming that E_2 (or S_3) has a low-affinity ($K_m \simeq 450$ μM) binding site for ATP that had to be occupied before the transition could occur. Although these experimental results were originally interpreted in terms of the Post-Albers scheme (E_2 to E_1), these results are actually much more consistent with the simultaneous model. In the Post-Albers scheme, the enzyme must go through the transition from E_2 to E_1 during Na-K exchange and one would predict from the above rate measurements that this transition would become rate-limiting at low [ATP]. However, since Na^+ is not involved in this transition, this would imply that the Na^+ dependence would decrease as the ATP concentration decreased. Quantitatively, the Na-K exchange reaction for the Post-Albers scheme can be described by:

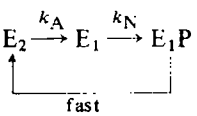

This would be a good approximation if K^+ were present and phosphate absent (so that dephosphorylation ($E_1P \rightarrow E_2$) is fast and irreversible). It will be assumed that the rate constant k_A is roughly proportional to the ATP concentration (a_A) and that k_N has a simple Michaelis-Menten dependence on the internal [Na^+] (a_N):

$$k_A = \alpha_A a_A \; ; \quad k_N = \alpha_N a_N/(a_N + K_N) \tag{10}$$

Solving for the overall rate of Na-K exchange:

$$J_{NK}/S = Va_N/(a_N + K_N^{ap})$$

$$K_N^{ap}/K_N = \alpha_A a_A/(\alpha_N + \alpha_A a_A) \simeq \underset{\text{low}\ [ATP]}{\alpha_A a_A/\alpha_N} \qquad (11)$$

Thus, it can be seen that the apparent K_m (K_N^{ap}) for Na^+ should increase approximately proportional to the ATP concentration (a_A) if the Post-Albers scheme is correct. This is not observed experimentally [45–48]. Flashner and Robinson [48] examined the widest range of ATP concentrations and found that K_m for Na^+ was about 13 mM at 6 μM ATP and about 5 mM at 3000 μM ATP. This appears to be a clear contradiction to the prediction of the Post-Albers scheme. In contrast, there is no contradiction with the simultaneous scheme proposed in this paper, since the transition rate that is being measured by the tryptophan fluorescence is from S_3 to S_4, which is by-passed during Na-K exchange when there is a direct transition from S_3 to S_1. Since the transition from S_3 to S_1 depends on the binding of Na^+ to S_3, one would predict that the K_m for Na^+ of the $(Na^+ + K^+)$-ATPase activity would be relatively independent of the ATP concentration, in agreement with the experimental results.

A similar type of argument can be applied to the reverse transition: E_1 to E_2 in the Post-Albers scheme or S_4 to S_3 in the simultaneous model. It has been shown by the use of formycin triphosphate binding that this transition varies linearly with the $[K^+]$ (up to at least 15 mM) and is very fast [38]. For example, at 10 mM K^+ this transition rate is about 60 s^{-1} which is about twice the maximal turnover rate of the $(Na^+ + K^+)$-ATPase measured under similar conditions [45]. Since the rate of Na-K reversal is only about 1/10 of this maximal turnover rate, the transition from E_1 to E_2 at 10 mM K^+ should be about 20-times faster than the overall rate of Na-K reversal. Since the E_1 to E_2 transition is the only step in the Post-Albers scheme that depends on the internal $[K^+]$, one would predict that the rate of Na-K reversal should be independent of the internal $[K^+]$ for concentrations greater than about 1 mM. However, Robinson et al. [22] have shown that the rate of Na-K reversal increases by more than 5-fold when the internal $[K^+]$ is increased from 10 to 100 mM – a clear disagreement with the predictions of the Post-Albers scheme. The experimental results are in agreement with the simultaneous model (Figs. 2 and 3A), since the fast transition corresponds to the transition from S_4 to S_3, while the rate-limiting step in Na-K reversal corresponds to the transition from S_1 to S_3 which is K^+ dependent.

The third case, which was discussed briefly in subsection IVB, is based on a comparison of the rates of Na-Na exchange and Na-K reversal. In the Post-Albers scheme, Na-K reversal involves cycling though the enzyme states in the backward direction:

$$E_1 \leftarrow E_1P \leftarrow E_2P \leftarrow E_2$$

As discussed above, the formycin triphosphate studies show that the reaction E_1 to E_2 is very fast [38]. Also, the phosphate-oxygen exchange experiments (see Section V) show that the E_2 to E_2P reaction step is also very fast [40]. Therefore, the reactions $E_2P \rightarrow E_1P \rightarrow E_1$ must be rate-limiting and responsible for the very slow rate that is observed for Na-K reversal. In the Post-Albers scheme, Na-Na exchange must involve the following reaction cycle:

$$E_1 \rightarrow E_1P \rightarrow E_2P \rightarrow E_1^*P$$

where the asterisk indicates that the occluded Na^+ is from the external medium. Since the reaction $E_2P \rightarrow E_1P \rightarrow E_1$ is also in this cycle, the Post-Albers scheme predicts that Na-K exchange and Na-K reversal should be limited by the same reaction steps and have roughly the same rate. However, at 150 mM internal [K^+], the observed maximum rate of Na-Na exchange [14] is about 10-times larger than that for Na-K reversal [49]. (The difference in rates is greater at lower internal K^+ concentrations.) Qualitatively, this relatively faster rate for Na-Na exchange is just what would be predicted for the simultaneous model where it is assumed that the rate-limiting step in Na-K reversal is the transition from S_1 to S_3 in which there is a positive free energy change and is therefore slow. In contrast, the rate-limiting step for Na-Na exchange is the transition α_N in Scheme II in which one subunit becomes phosphorylated while the other subunit is simultaneously dephosphorylated – a reaction which is relatively fast, since the free energy change is zero. The following argument may help to explain the difference in the two models. For Na-K reversal, the rate-limiting process for both models is the step corresponding to E_1P to E_1 which, presumably, has a positive free energy change and is therefore slow. For Na-Na exchange, in the sequential Post-Albers scheme the same step is rate-limiting, while in the simultanous model this slow step is driven by the simultaneous phosphorylation of the other subunit. It is shown in Section IV that the quantitative predictions of the simultaneous model agree with the observed dissociation constants for internal K^+ during K^+-K^+ exchange and Na-K reversal.

Finally, an intriguing piece of evidence in support of this simultaneous model comes from experiments in which the enzyme is modified by treatment with either digitonin [50] or mercurials [51,52]. Although this treatment inhibits the ($Na^+ + K^+$)-ATPase activity of the enzyme, it leaves relatively unaltered partial reactions such as ATP-ADP exchange, Na^+-ATPase, the rate of Na^+-stimulated phosphorylation and K^+-stimulated dephosphorylation and K^+ phosphatase activity. Since there is some evidence that these modifications uncouple the enzyme dimer, it is of interest to see how the model proposed here (Figs. 2 and 3A) would behave if the two subunits were uncoupled. The only step in the cycle where the subunits are coupled is the transition from S_3 to S_1 or S_3 to S_4. During the coupled reaction, the free energy released when subunit D is phosphorylated (S_3 to S_1) or has ATP bind to it with a high affinity (S_3 to S_4) is used to drive the energetically unfavorable transition of subunit C to D. If the enzyme were uncoupled and K^+ present, then all the enzyme would end up locked in state C (inhibited). However, in the absence of K^+, the enzyme could undergo the normal transitions from state A to C and one would expect that ATP-ADP exchange and Na^+-ATPase (which are measured in zero [K^+]) would be relatively normal. Also, the K^+ phosphatase activity should be relatively normal, since it is probably associated either with state C or the transition between states B and C [53]. Thus, the predictions of the model are in perfect agreement with the experimental behavior that is observed for the presumably uncoupled enzyme. If this relationship could be clearly established then these modifiers would provide definitive evidence for a simultaneous model and would become important tools for investigating the pump mechanism.

Appendix

AI. Solution to Scheme I (state S_4 neglected)

AIA. Na-K exchange (J_{NK})

The general solution for the net rate of turnover (J) through the cycle of Scheme I is given by [54]:

$$J/S = \frac{k_1 k_2 k_3 - k_{-1} k_{-2} k_{-3}}{k_2(k_3 + k_1 + k_{-3}) + k_{-1}(k_{-2} + k_3 + k_{-3}) + k_{-3}(k_{-1} + k_{-2} + k_2)} \tag{1A}$$

where S is the total amount of enzyme present and the k terms are the rate constants shown in Scheme I. The second term in the numerator of Eqn. 1A ($k_{-1}k_{-2}k_{-3}$) represents the rate of Na-K reversal and is negligible under conditions where Na-K exchange can occur. In the denominator, k_2 and k_{-1} are functions of the external concentrations of Na (a_N^o) and K (a_K^o) while k_3 and k_{-3} are functions of the internal concentrations of Na (a_N^i) and K (a_K^i). It can be seen that in order for Eqn. 1A to be of the form of Eqn. 1 it is necessary to assume that:

$$(k_3 \text{ and } k_{-3}) << (k_1 \text{ and } k_{-2}) \tag{2A}$$

Then, for Na-K exchange (J_{NK}), Eqn. 1A reduces to:

$$J_{NK}/S = k_1 k_2 k_3 / D \tag{3A}$$

$$D = k_2 k_1 + k_{-1} k_{-2} + k_1 k_{-2}$$

The rate of the transition from S_3 to S_1 is described by:

$$k_3 S_3 = \alpha_3 S_3^N \tag{4A}$$

where S_3^N is the state S_3 when the channel exposed to the internal solution (state D, Fig. 1) is occupied by three Na^+. The rate constant α defined as in Eqn. 4A is concentration independent. The state S_3^N can be related to S_3:

$$S_3^N = f(a_N^i | a_K^i) S_3 \tag{5A}$$

where f is the probability that S_3 is in state S_3^N. Combining Eqns. 5A and 4A:

$$k_3 = \alpha_3 f(a_N^i | a_K^i) \tag{6A}$$

Similarly:

$$k_{-3} = \alpha_{-3} r(a_K^i | a_N^i); \quad k_2 = \alpha_2 g(a_K^o | a_N^o); \quad k_{-1} = \alpha_{-1} h(a_N^o | a_K^o) \tag{6A}$$

Substituting Eqns. 5A and 6A into Eqn. 3A, one obtains the general expression used in the text (Eqn. 2) for Na-K exchange:

$$J_{NK}/S = \alpha_1 \alpha_2 \alpha_3 f(a_N^i | a_K^i) g(a_K^o | a_N^o) / D(a_K^o, a_N^o)$$

where

$$D = \alpha_1 \alpha_{-2} + \alpha_2 \alpha_1 g(a_K^o | a_N^o) + \alpha_{-1} \alpha_{-2} h(a_N^o | a_K^o) \tag{7A}$$

In most cases, k_{-1} is very small so that Eqn. 7A can be approximated by:

$$J_{NK}/S = \frac{\alpha_2 \alpha_3 f g}{\alpha_2 g + \alpha_{-2}} \tag{8A}$$

AIB. Na-K reversal (J_R)

Reversal is measured experimentally by making $a^o_K = 0$ so that $k_2 = 0$. Using this condition in Eqn. 1A:

$$J_R/S = \alpha_{-1}\alpha_{-2}\alpha_{-3}r(a^i_K|a^i_N)h(a^o_N|a^o_K)/D(a^o_N, a^o_K) \tag{9A}$$

AIC. Na-Na exchange (J_{NN})

From Scheme II of the text it is easy to show that the rate of Na-Na exchange is described by:

$$J_{NN}/S = \alpha_N S^N_1/S = \alpha_N f(a^i_N|a^i_K)S_1/S \tag{10A}$$

In general:

$$S_1/S = \frac{k_{-2}k_{-1} + k_{-1}k_3 + k_2k_3}{D} \tag{11A}$$

Experimentally, Na-Na exchange is measured under conditions where $a^o_K = 0$ ($k_2 = 0$) and using Eqn. 2A:

$$\frac{S_1}{S} = \frac{k_{-1}k_{-2}}{D} \tag{12A}$$

Combining Eqns. 10A and 12A:

$$J_{NN}/S = \alpha_N\alpha_{-1}\alpha_{-2}f(a^i_N|a^i_K)h(a^o_N|a^o_K)/D(a^o_N, a^o_K) \tag{13A}$$

AII. Solution with state S_4 included

The kinetics are now described by the following scheme:

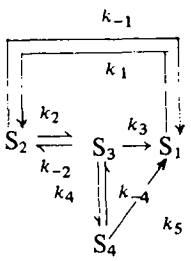

Scheme IVA.

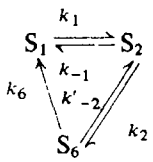

Scheme IVB.

where it has been assumed that k_{-3} and k_{-5} are small and can be neglected. Scheme IVB is equivalent to IVA with the following relationships:

$$S_6 = S_3 + S_4\ ; \quad k_{-2}S_3 = k'_{-2}S_6\ ; \quad k_6S_6 = k_3S_3 + k_5S_4 \tag{14A}$$

Also:

$$k_4S_3 = (k_{-4} + k_5)S_4 \tag{15A}$$

Combining Eqns. 14A and 15A:

$$k'_{-2} = \frac{k_{-2}}{1+\gamma}\ ; \quad k_6 = \frac{k_3 + \gamma k_5}{1+\gamma}\ ; \quad \gamma = \frac{k_4}{k_{-4} + k_5} \tag{16A}$$

Scheme IVB is of the same form as Scheme I and has the same general solution.

AIIA. K-K exchange (J_{KK})

It can be seen from Scheme III that the rate of K-K exchange is described by:

$$J_{KK}/S = \frac{k_{-4}S_4}{S} \tag{17A}$$

$$S_4 = \frac{\gamma}{1+\gamma} S_6 \quad \text{and} \quad S_6 = \frac{k_1 k_2 + k_{-1}k_{-3} + k_2 k_{-3}}{D'} \tag{18A}$$

Where D' is D (e.g., Eqn. 3A) with k'_{-2} substituted for k_{-2}.
The general solution for K-K exchange is given by:

$$J_{KK}/S = \frac{k_{-4}\gamma k_1 k_2}{(1+\gamma)D'} \tag{19A}$$

For the special case where the internal $[Na^+]$ is zero ($k_3 = k_5 = k_6 = 0$) and external $[K^+]$ is large ($k_2 >> k_{-2}$) and k_{-1} is small:

$$J_{KK}/S = \frac{k_{-4}\alpha_4}{k_{-4} + \alpha_4} \qquad k_{-4} = \alpha_{-4} r(a_K^i | a_N^i) \tag{20A}$$

where it has been assumed that k_{-3} and k_{-4} have the same dependence on the K^+ concentration.

AIIB. Kinetics of Na-K exchange when the internal $[K^+] = 0$

Sachs [19] showed that when $a_K^i = 0$, the apparent affinity for external K^+ varied with the internal $[Na^+]$. This is a contradiction to Eqn. 1. It will be shown here that this result is consistent with the model. When $a_K^i = 0$, $k_{-4} = 0$ and $\gamma = k_4/k_5$. Since Scheme IVB is of the same form as Scheme I, the general solution for Na-K exchange is described by Eqn. 3A with k'_{-2} and k_6 substituted for k_2 and k_3, respectively (assume k_{-1} is small):

$$J_{NK}/S = \frac{k_2 k_6}{k_2 + k'_{-2}} = \frac{k_6 \alpha_2 g(a_K^o | a_N^o)}{\alpha_2 g + k'_{-2}} \tag{21A}$$

Assume that g has a simple Michaelis-Menten form:

$$g = a_K^o/(a_K^o + K_K) \tag{22A}$$

Then:

$$J_{NK}/S = V a_K^o/(a_K^o + K_K^{ap}) \tag{23A}$$

$$V = k_6 \alpha_2/(\alpha_2 + k'_{-2})$$

$$K_K^{ap}/K_K = k'_{-2}/(\alpha_2 + k'_{-2})$$

It can be seen that the apparent affinity for external K^+ (K_K^{ap}) is a function of the interval $[Na^+]$, since it is a function of k_4 (through k'_{-2}) which depends on the internal $[Na^+]$. If the internal $[K^+]$ is high (above about 10 mM) as is the usual case, then $\gamma << 1$ and K_K^{ap} is no longer a function of the internal $[Na^+]$.

The predictions of the model are in rough quantitative agreement with the results of

Sachs. Assuming that f (Eqn. 6A) is of the same form as Eqn. 22A, then from Eqn. 23A:

$$\frac{V}{K_K^{ap}} = \frac{\alpha_2\alpha_3}{K_K\alpha_{-2}}\left(\frac{a_N}{a_N + K_N} + \frac{\alpha_4}{\alpha_3}\right) \tag{24A}$$

Eqn. 24A can be fitted to the data of Sachs if: (1) $\alpha_4/\alpha_3 \ll 1$; (2) K_N (the affinity of state D for Na^+) $\simeq 1$ mM; and (3) $\alpha_2\alpha_3/(K_K\alpha_{-2}) \simeq 13\,l^{-1}$. Using these conditions, it is necessary to assume that the affinity of state E for Na^+ is greater than about 10 mM in order to fit the dependence of K_K^{ap} on a_N^i that was found by Sachs.

AIII. Kinetics when multiple occupancy states of the external site are included

The kinetics are now described by the following scheme (assuming $k_{-1} = k_{-3} = 0$):

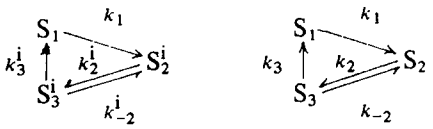

Scheme V. Scheme I.

In Scheme V, S_2^i and S_3^i refer to the different occupancy conditions of state B (Fig. 4) and the corresponding state C, respectively. For each occupancy state, there are a different set of rate constants k_2^i, and k_3^i. The solution to Scheme V is based on relating it to Scheme I as follows. Define:

$$S_2^i = p_i S_2 \; ; \quad S_3^i = q_i S_3 \tag{25A}$$

Also:

$$k_2 S_2 = (k_3 + k_{-2})\, S_3 \Rightarrow S_3 = MS_2$$

where

$$M = \frac{k_2}{k_3 + k_{-2}} \simeq \frac{k_2}{k_{-2}}$$

$$k_2^i S_2^i = (k_3^i + k_{-2}^i)\, S_3^i \Rightarrow S_3^i = M_i S_2^i = M_i p_i S_2 = \frac{M_i p_i}{M}\, S_3 \tag{26A}$$

Comparing Eqns. 25A and 26A:

$$q_i = \frac{M_i p_i}{M} \; ; \qquad \Sigma q_i = 1 \Rightarrow M = \Sigma M_i p_i \tag{27A}$$

In general, the rate of K^+ transport into the cell (J_K) is described by:

$$J_K = \Sigma n_i k_3^i S_3^i = S_3\, \Sigma n_i k_3^i q_i \tag{28A}$$

From the solution to Scheme I:

$$\frac{S_3}{S} = \frac{k_2}{k_2 + k_{-2}} \simeq \frac{M}{1 + M} \tag{29A}$$

Substituting Eqns. 29A and 27A in Eqn. 30A, the final expression for J_K is obtained:

$$J_K/S = \frac{\Sigma n_i k_3^i p_i M_i}{1 + M} \tag{30A}$$

The occupancy conditions of state B (Fig. 4) are related to each other through the following state diagram:

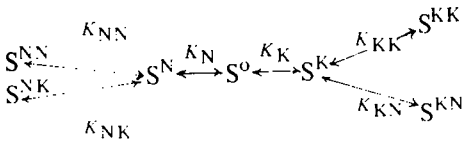

(31A)

The K terms are equilibrium constants which can be related to the probabilities (p_i) of being in the different states:

$$p_o = 1/A \; ; \quad p_K = K_K a_K/A \; ; \quad p_{KK} = K_K K_{KK} a_K^2/A \; ; \quad p_{KN} = K_K K_{KK} a_N a_K/A \tag{32A}$$

$$p_N = K_N a_N/A \; ; \quad p_{NN} = K_N K_{NN} a_N^2/A \; ; \quad p_{NK} = K_N K_{NK} a_N a_K/A$$

The expression for A is determined from the condition:

$$\Sigma p_i = 1 \tag{33A}$$

and is therefore equal to the sum of the numerators in Eqn. 32A. The main assumption of the model is that dephosphorylation (k_2) cannot occur if an Na^+ is at the central site. Thus, k_2^i and M_i are zero for the states S^{NN}, S^N and S^{NK}. To simplify the discussion, the K^+ flux (Eqn. 30A) will be examined for various concentration regimes.

AIIIA. High [Na⁺], varying [K⁺]

High $[Na^+]$ means that $K_N a_N >> 1$ and therefore the only terms that contribute to Eqn. 30A are:

$$A \simeq K_N a_N + K_K K_{KK} a_K^2$$

$$M = \Sigma M_i p_i \simeq M_{KK} p_{KK}$$

$$J_K/S = \frac{2k_3^{KK} p_{KK} M_{KK}}{1 + M_{KK} p_{KK}} = \frac{2k_3^{KK} K_K K_{KK} M_{KK} a_K^2}{K_N a_N + K_K K_{KK}(1 + M_{KK}) a_K^2} \tag{34A}$$

Eqn. 34A has the sigmoid dependence on the external K^+ concentration (a_K) that has been well established experimentally.

AIIIB. Zero external [Na⁺] with varying external [K⁺]

For these conditions:

$$M = M_o p_o + M_K p_K + M_{KK} p_{KK} \; ; \quad E = 2k_3^{KK} M_{KK} K_{KK}/(k_3^K M_K)$$

$$A = 1 + a_K K_K + a_K^2 K_K K_{KK} \tag{35A}$$

$$J_K/S = \frac{k_3^K M_K K_K (1 + E a_K) a_K}{(1 + M_o) + (1 + M_K) K_K a_K + (1 + M_{KK}) K_{KK} K_K a_K^2}$$

Eqn. 35A for J_K is of the same general form as that derived by Sachs [33]. Sachs showed that, depending on the relative values of the constants, this dependence of the flux on the external $[K^+]$ could be a sigmoid, anti-sigmoid or a rectangular hyperbola, in agreement with experimental observations.

AIIIC. Flux as a function of the external [Na^+]

For the original model of Sachs, a plot of J_K^{-1} vs. the external [Na^+] (a_N) should be linear. Sachs showed that this was found experimentally at moderate levels of external K^+. However, Cavieres and Ellory [35] showed that at very low levels of external K^+, this plot tended to bend towards the horizontal (a_N) axis. The model proposed here can also explain this curvature. For the general case, J_K^{-1} can be written in the form:

$$J_K^{-1} = [F(a_K) + G(a_K)\,a_N]/[H(a_K) + I(a_K)\,a_N] \qquad (36A)$$

The second term in the denominator of Eqn. 36A arises from the state S^{KN} for which one K^+ and one Na^+ are transported into the cell per cycle. This is a new feature of this model. At moderate values of [K^+], this term is negligible compared to $H(a_K)$ and the plot is linear in a_N. However, at very low K^+ concentrations, this term becomes significant and the plot tends to level off, as is observed experimentally.

Acknowledgements

I wish to thank Drs. Jack Kaplan and Robert Post for critically reading and commenting on this manuscript. This work was supported in part by NIH grant 5R01GM25938.

References

1 Robinson, J.D. and Flashner, M.S. (1979) Biochim. Biophys. Acta 549, 145–176
2 Cavieres, J.D. (1977) in Membrane Transport in Red Cells (Ellory, J.C. and Lew, V.L., eds.), pp. 1–37, Academic Press, London
3 Glynn, I.M. and Karlish, S.J.D. (1975) Annu. Rev. Physiol. 37, 13–55
4 Skou, J.C. and Norby, J.G. (1979) Na, K-ATPase – Structure and Kinetics, Proceedings of the 2nd International Conference on the Properties and Functions of Na, K-ATPase, Academic Press, London
5 Post, R.L. (1977) in Biochemistry of Membrane Transport (Semenza, G. and Carafoli, E., eds.), FEBS Symp. No. 42, pp. 352–362, Springer-Verlag, Berlin
6 Levitt, D.G. (1978) Biophys. J. 22, 209–219
7 Levitt, D.G. (1978) Biophys. J. 22, 221–248
8 Garrahan, P.J. and Glynn, I.M. (1967) J. Physiol. 192, 217–235
9 Hilden, S. and Hokin, L.E. (1975) J. Biol. Chem. 250, 6296–6303
10 Sweadner, K.J. and Goldin, S.M. (1975) J. Biol. Chem. 250, 4022–4024
11 Goldin, S.M. (1977) J. Biol. Chem. 252, 5630–5642
12 Anner, B.M., Lane, K.K., Schwartz, A. and Pitts, B.J.R. (1977) Biochim. Biophys. Acta 476, 340–345
13 Bowman, R.J. and Levitt, D.G. (1977) Biochim. Biophys. Acta 466, 68–83
14 Garay, R.P. and Garrahan, P.J. (1973) J. Physiol. 231, 297–325
15 Taniguchi, K. and Post, R.L. (1975) J. Biol. Chem. 250, 3010–3018
16 Mardh, S. and Lindahl, S. (1977) J. Biol. Chem. 252, 8058–8061
17 Karlish, S.J.D., Yates, D.W. and Glynn, I.M. (1978) Biochim. Biophys. Acta 525, 252–264
18 Warshel, A. (1978) Proc. Natl. Acad. Sci. U.S.A. 75, 5250–5254
19 Sachs, J.R. (1977) J. Physiol. 273, 489–514
20 Hoffman, P.G. and Tosteson, D.C. (1971) J. Gen. Physiol. 58, 438–466
21 Garrahan, P.J. and Garay, R.P. (1976) Curr. Top. Membrane Transp. 8, 29–97
22 Robinson, J.D., Hall, E.S. and Dunham, P.B. (1977) Nature 269, 165–167
23 Chipperfield, A.R. and Whittam, R. (1976) J. Physiol. 260, 371–385
24 Garay, R.P. and Garrahan, P.J. (1975) J. Physiol. 249, 51–67
25 Robinson, J.D., Flashner, M.S. and Marin, G.K. (1978) Biochim. Biophys. Acta 509, 419–428
26 Glynn, I.M., Hoffman, J.F. and Lew, V.L. (1971) J. Physiol. 218, 239–256

27 Cavieres, J. and Glynn, I.M. (1979) J. Physiol. 297, 637–645
28 Simons, T.J.B. (1974) J. Physiol. 237, 123–155
29 Robinson, J.D. (1976) Biochim. Biophys. Acta 429, 1006–1019
30 Simons, T.J.B. (1975) J. Physiol. 244, 731–739
31 Mardh, S. and Post, R.L. (1977) J. Biol. Chem. 252, 633–638
32 Beauge, L.A. and Glynn, I.M. (1979) J. Physiol. 289, 17–31
33 Sachs, J.R. (1977) J. Physiol. 264, 449–470
34 Sachs, J.R. (1967) J. Clin. Invest. 46, 1433–1441
35 Cavieres, J.D. and Ellory, J.C. (1975) Nature 255, 338–340
36 Glynn, I.M. and Karlish, S.J.D. (1976) J. Physiol. 256, 465–496
37 Hegyvary, C. and Post, R.L. (1971) J. Biol. Chem. 246, 5234–5240
38 Karlish, S.J.D., Yates, D.W. and Glynn, I.M. (1978) Biochim. Biophys. Acta 525, 252–264
39 Mardh, S. (1975) Biochim. Biophys. Acta 391, 464–473
40 Dahms, A.S. and Boyer, P.D. (1973) J. Biol. Chem. 248, 3155–3162
41 Karlish, S.J.D. and Yates, D.W. (1978) Biochim. Biophys. Acta 527, 115–130
42 Karlish, S.J.D. (1979) in Na, K-ATPase – Structure and Kinetics (Skou, J.C. and Norby, J.G., eds.), pp. 115–128, Academic Press, London
43 Mardh, S. and Zetterqvist, O. (1974) Biochim. Biophys. Acta 350, 473–483
44 Lowe, A.G. and Smart, J.W. (1977) Biochim. Biophys. Acta 481, 695–705
45 Hexum, T., Samson, F.E. and Himes, R.H. (1970) Biochim. Biophys. Acta 212, 322–331
46 Peter, H.W. and Wolf, H.U. (1972) Biochim. Biophys. Acta 290, 300–309
47 Wang, T., Lindenmayer, G.E. and Schwartz, A. (1977) Biochim. Biophys. Acta 484, 140–160
48 Flashner, M.S. and Robinson, J.D. (1979) Arch. Biochem. Biophys. 192, 584–591
49 Garrahan, P.J. and Glynn, I.M. (1967) J. Physiol. 192, 237–256
50 Winter, C.G. and Moss, A.J. (1979) in Na, K-ATPase – Structure and Kinetics (Skou, J.C. and Norby, J.G., eds.), pp. 25–32, Academic Press, London
51 Askari, A., Huang, W. and Henderson, G.R. (1979) in Na, K-ATPase – Structure and Kinetics (Skou, J.C. and Norby, J.G., eds.), pp. 205–216, Academic Press, London
52 Hansen, O., Jensen, J. and Ottolenghi, P. (1979) in Na, K-ATPase – Structure and Kinetics (Skou, J.C. and Norby, J.G., eds.), pp. 217–226, Academic Press, London
53 Post, R.L., Hegyvary, C. and Kume, S. (1972) J. Biol. Chem. 247, 6530–6540
54 Segal, I.H. (1975) Enzyme Kinetics, John Wiley and Sons, Inc., New York
55 Neufeld, A.H. and Levy, H.M. (1969) J. Biol. Chem. 244, 6493–6497
56 Kanazawa, T., Saito, M. and Tonomura, Y. (1970) J. Biochem. 67, 693–711